bioRxiv preprint doi: https://doi.org/10.1101/038513; this version posted February 2, 2016. The copyright holder for this preprint (which was not certified by peer review) is the author/funder. All rights reserved. No reuse allowed without permission.

ERK5 kinase activity is not required for cellular immune response

Emme C.K. Lin[1*], Christopher M. Amantea[1], Tyzoon K. Nomanbhoy[1], Helge Weissig[1], Junichi Ishiyama[2], Yi Hu[1], Shyama Sidique[1], Bei Li[1], John W. Kozarich[1], Jonathan S. Rosenblum[1]

[1]ActivX Biosciences, Inc., La Jolla, CA, United States of America

[2]Watarase Research Center, Kyorin Pharmaceutical Co., Ltd., Nogi, Nogi-machi, Shimotsuga-gun, Tochigi, Japan

bioRxiv preprint doi: https://doi.org/10.1101/038513; this version posted February 2, 2016. The copyright holder for this preprint (which was not certified by peer review) is the author/funder. All rights reserved. No reuse allowed without permission.

Abstract

Extracellular signal-regulated protein kinase 5 (ERK5) has been associated with several pathological states including cancer, cardiac hypertrophy, and inflammation. Unlike other members of the MAPK family, ERK5 contains a large C-terminal domain with transcriptional activation capability. Pharmacological inhibition of ERK5 with XMD8-92, a first generation ERK5 inhibitor, is efficacious in various oncology and inflammation models. Here we report the synthesis and characterization of potent and selective ERK5 inhibitors. Most of these compounds displayed good efficacy in cellular inflammation assays; intriguingly, other compounds lacked efficacy despite potently inhibiting ERK5 in vivo. The source of XMD8-92 and related compounds' efficacy is now demonstrated to be from direct inhibition of bromodomains (BRDs), conserved protein modules involved in recognition of acetyl-lysine residues during transcriptional processes. We found no cellular effect from pure ERK5 inhibitors and conclude that ERK5 kinase activity is not required for the immune response. The role of ERK5 in inflammation and oncology should be reinvestigated.

bioRxiv preprint doi: https://doi.org/10.1101/038513; this version posted February 2, 2016. The copyright holder for this preprint (which was not certified by peer review) is the author/funder. All rights reserved. No reuse allowed without permission.

Introduction

Extracellular signal-regulated kinase 5 (ERK5) is a member of the mitogen-activated protein kinase (MAPK) family, which includes ERK1/2, JNK1/2/3, and p38α/β/δ/γ[1]. Originally named big mitogen activated protein kinase 1 (BMK1) due to its uniquely large, 400 amino acid C-terminal domain, ERK5 can be phosphorylated as a result of cellular exposure to a broad range of mitogenic stimuli (e.g., growth factors, GPCR agonists, cytokines) and cellular stresses (e.g., hypoxia, shear stress)[2]. Through the MAPK signaling cascade, ERK5 can undergo dual phosphorylation by MEK5 at the TEY motif in its N-terminal activation loop, resulting in conformation change and unlocking full kinase activity [3]. ERK5 can auto-phosphorylate multiple sites in its C-terminal half, which can then regulate nuclear shuttling and gene transcription[4,5]. Non-canonical kinase pathways (including cyclin dependent kinases during mitosis and ERK1/2 during growth factor stimulation) also exist for phosphorylation of overlapping sites in the ERK5 tail[6–8]. While ERK5 has been demonstrated to directly phosphorylate several transcription factors[9–11], the non-kinase C-terminal tail of ERK5 can also interact with transcription factors and influence gene expression via its transcriptional activation domain[5,12,13].

ERK5 deletion is embryonic lethal in mice and a variety of tissue or development-stage restricted deletions have shown clear, yet diverse phenotypes, suggesting that the kinase function and/or an aspect of the non-kinase domain(s) have key roles in development[14–18]. The recent description of the first ERK5 inhibitor XMD8-92 allowed for selectively studying the role of ERK5 kinase activity[19,20]. Effects of this inhibitor on cell proliferation were shown to be comparable to overexpression of a dominant negative ERK5 mutant[20,21] or to siRNA-mediated ERK5 knockdown[21,22]. Following a recent report on the role of ERK5 in TLR2-mediated

bioRxiv preprint doi: https://doi.org/10.1101/038513; this version posted February 2, 2016. The copyright holder for this preprint (which was not certified by peer review) is the author/funder. All rights reserved. No reuse allowed without permission.

inflammation[23], we set out to develop additional potent and selective ERK5 inhibitors as anti-inflammatory agents. Analysis of these new inhibitors, and further characterization of first generation ERK5 inhibitors, shows that ERK5 kinase activity is dispensable for immunity.

bioRxiv preprint doi: https://doi.org/10.1101/038513; this version posted February 2, 2016. The copyright holder for this preprint (which was not certified by peer review) is the author/funder. All rights reserved. No reuse allowed without permission.

Results

Inhibitors of ERK5

Our interest in the pharmacological regulation of ERK5 in inflammation led to the development of a number of novel ERK5 kinase inhibitors derived from the benzopyrimidodiazepinone core of XMD8-92 (**Fig. 1**). The ATP-competitive inhibitors were shown to potently inhibit ERK5 with IC_{50} values ranging from 8 to 190 nM using our chemoproteomics platform KiNativ, which profiles global kinase inhibition in native cellular lysates[24,25]. Using a 1 μM screening concentration, we did not observe significant inhibition of off-target kinase activities among the greater than 100 kinases profiled in a single cellular lysate (Supplementary Results, **Supplementary Data Set 1**).

bioRxiv preprint doi: https://doi.org/10.1101/038513; this version posted February 2, 2016. The copyright holder for this preprint (which was not certified by peer review) is the author/funder. All rights reserved. No reuse allowed without permission.

Figure 1. Compound structures and potencies against ERK5 in cell lysate and in live cells treated with compound.

Compound	Structure	Lysate ERK5 IC_{50} (nM)	Intracellular ERK5 IC_{50} (nM)
AX15836 (**A10**)	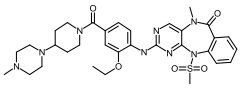	8	9
AX15839 (**B8**)	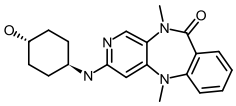	170	430
AX15892 (**C7**)	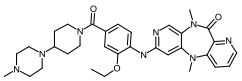	30	110
AX15910 (**B11**)	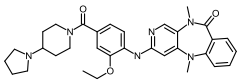	20	17
XMD8-92	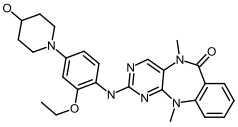	190	130

bioRxiv preprint doi: https://doi.org/10.1101/038513; this version posted February 2, 2016. The copyright holder for this preprint (which was not certified by peer review) is the author/funder. All rights reserved. No reuse allowed without permission.

The ERK5 inhibitors were also evaluated in an additional KiNativ experiment ("live cell KiNativ") wherein compound is incubated with live cells prior to washing, lysis and analysis. Such experiments provide an indication of the cellular permeability of the compound and of intracellular target- (and off target-) engagement. As seen in **Fig. 1**, intracellular ERK5 IC_{50} values were very similar to lysate ERK5 IC_{50} values, thus demonstrating that the compounds effectively reached their intracellular target.

The compounds were next tested for their ability to inhibit EGF-mediated autophosphorylation of ERK5 in HeLa cells[5]. In this classical band shift assay, growth factor stimulation results in the appearance of a slower migrating, autophosphorylated ERK5 form[26]. As seen in **Fig. 2**, when treated at 2 μM, a concentration of at least 10-fold over the weakest ERK5 IC_{50}, all of the ERK5 inhibitors substantially blocked the mobility-retarded phosphorylated ERK5 band as expected. This phospho-ERK5 data together with the live cell KiNativ results indicated that we had potent, selective ERK5 inhibitors that were able to effectively engage their intracellular target.

bioRxiv preprint doi: https://doi.org/10.1101/038513; this version posted February 2, 2016. The copyright holder for this preprint (which was not certified by peer review) is the author/funder. All rights reserved. No reuse allowed without permission.

Figure 2. Hela cell autophosphorylation assay.

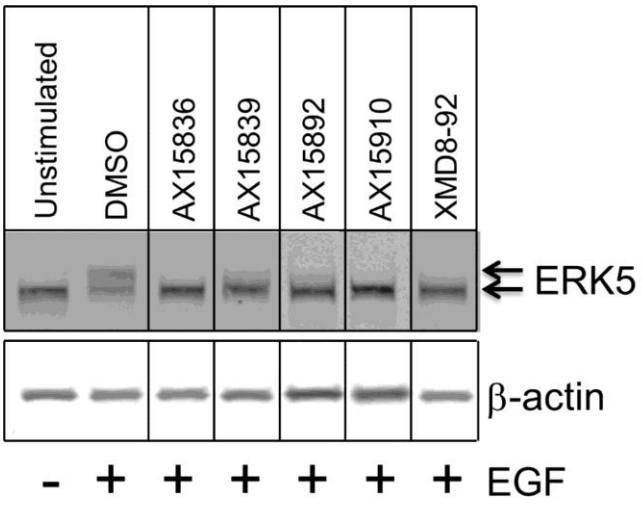

Stimulation of HeLa cells with EGF induced a slower migrating, autophosphorylated ERK5 band (upper arrow) whose appearance was prevented by pharmacological ERK5 inhibition. Compounds were screened at 2 μM. Figure is a composite of lanes from nonadjacent samples.

Characterization of inhibitors in inflammatory cell models

We next assessed the ERK5 compounds in a cellular assay of inflammatory response. To function in the recruitment of neutrophils and monocytes, the endothelial cell adhesion molecule E-selectin is rapidly synthesized in response to inflammatory stimulation[27]. Primary human umbilical vein endothelial cells (HUVEC) were incubated with compounds prior to stimulation with the toll-like receptor (TLR1/2) agonist Pam_3CSK_4, a synthetic mimic of the acylated amino terminus of bacterial triacylated lipopeptides. Up-regulation of cell-surface E-selectin was quantified by flow cytometry (**Table 1**). Similar to that reported by Wilhelmsen and colleagues[23], we found the ERK5 inhibitor XMD8-92 to inhibit up to 38% of the E-selectin expression. Likewise, two other ERK5 inhibitors AX15839 and AX15910 were effective in reducing E-selectin. Surprisingly, two of the more potent ERK5 inhibitors (AX15836 and

bioRxiv preprint doi: https://doi.org/10.1101/038513; this version posted February 2, 2016. The copyright holder for this preprint (which was not certified by peer review) is the author/funder. All rights reserved. No reuse allowed without permission.

AX15892) were inactive in this assay, even at a concentration of compound at least 90-fold higher than the intracellular ERK5 IC_{50} (**Fig. 1**).

Given these results, it seemed likely that an additional activity was responsible for the efficacy of AX15839, AX15910, and XMD8-92. However, from KiNativ profiling, there were no significant shared kinase off-targets from the more than 200 kinases profiled, at up to 10 μM compound (Supplementary Results, **Supplementary Data Set 2**). XMD8-92 was derived from the polo-like kinase (PLK1) inhibitor BI-2536[19,20]. Recently, BI-2536 (as well as numerous other kinase inhibitors) has been shown to inhibit the interaction between bromodomain and acetyl-lysine binding[28–30]. Bromodomains (BRD) are protein modules that bind to ε-N-acetylated lysine-containing sequences and modulate transcriptional processes. In particular, the bromodomain-containing BET (bromo and extra terminal) proteins BRD2, BRD3, BRD4, and BRDT are targets of drugs currently pursued in oncology, diabetes, atherosclerosis, and inflammation. In order to determine whether XMD8-92 and other ERK5 kinase inhibitors can likewise inhibit BRDs, we screened the compounds against BRD4, a well-studied and key member of the BET protein family.

Table 2 shows the dissociation constants for compound binding to the frist bromodomain of BRD4 ((BRD4(1)). Using the well validated, q-PCR-based BROMOscan assay (DiscoveRx Corp., San Diego, CA), two reference BRD inhibitors, JQ1[31] and I-BET762[32] exhibited potent BRD4(1) K_d values that are concordant with published isothermal titration calorimetry results[31,33]. Analysis of the ERK5 inhibitors using this method revealed a clear split. Compounds that were active in the E-selectin assay, AX15839, AX15910 and XMD8-92, potently bound BRD4(1). In contrast, compounds that were potent on ERK5 but inactive in the E-selectin assay, AX15836 and AX15892, gave considerably higher dissociation constants.

bioRxiv preprint doi: https://doi.org/10.1101/038513; this version posted February 2, 2016. The copyright holder for this preprint (which was not certified by peer review) is the author/funder. All rights reserved. No reuse allowed without permission.

Knowing that the dual ERK5/BRD inhibitors were efficacious in the E-selectin HUVEC assay whereas the ERK5-selective inhibitors had no effect (**Table 1**), we returned to that assay to measure the two BRD-selective reference inhibitors. Using only 1 μM of I-BET762 and JQ1, we observed E-selectin reductions of 27 and 29%, respectively. Of note, neither BRD inhibitor had any significant kinase inhibition at up to 10 μM by KiNativ profiling (data not shown). Thus it appears that TLR1/2-induced E-selectin expression in endothelial cells could be reduced by BRD inhibition but not by ERK5 inhibition.

We characterized the activities of several compounds from each classification type in additional cellular inflammation models and found good consistency of response. For brevity, we show the results of three representative compounds: AX15836 as the ERK5-selective inhibitor, AX15839 as the dual ERK5/BRD inhibitor, and I-BET762 as the selective BRD inhibitor. HUVECs were pre-treated with compound and stimulated with TLR1/2 agonist Pam_3CSK_4. Culture supernatants were subjected to immunoassay for inflammatory cytokines IL-6 and IL-8. As seen in **Table 3**, compounds with BRD inhibition (selective and dual) suppressed IL-6 and IL-8; however, the ERK5-specific inhibitor AX15836 was completely ineffective (EC_{50}>>10μM), suggesting that it was the BRD inhibition component of the compounds that mediated cytokine reduction.

To determine whether the lack of ERK5-specific effect was limited to a certain cell type and agonist, we repeated the experiment using a normal human bronchial epithelial cell line, BEAS-2B. After pre-incubation with compound, cells were stimulated with the pro-inflammatory cytokine IL-17A under complete growth media conditions. Intriguingly, ERK5 has been identified to be part of an IL-17-mediated signaling cascade that drives keratinocyte proliferation and tumorigenesis[34]. IL-17A is also overexpressed in other conditions of chronic

bioRxiv preprint doi: https://doi.org/10.1101/038513; this version posted February 2, 2016. The copyright holder for this preprint (which was not certified by peer review) is the author/funder. All rights reserved. No reuse allowed without permission.

inflammation such as asthma and is thought to mediate airway neutrophilia through the induction of additional cytokines from target cells[35–37]. IL-6 and IL-8 cytokine release from the bronchial epithelial cells were measured by immunoassay (**Table 4**). Again, the ERK5-selective compound AX15836 had no effect on these induced cytokines. In contrast, inhibitors with BRD inhibition activity suppressed inflammatory cytokine response to IL-17A in this cell type.

We searched for an anti-inflammatory effect of AX15836 in additional cellular models of innate and adaptive immunity from both murine and human sources, as listed in **Supplementary Table 1**. Inhibition of BRD/acetyl-lysine binding with either JQ1 or I-BET762 resulted in efficacy across most models. In contrast, the ERK5-only inhibitor AX15836 was ineffective against all models tested.

Transcriptome analysis of cellular ERK5 kinase inhibition

Since we were unable to find effects of ERK5 inhibitor treatment on a limited number of analytes previously reported to be modulated by compounds now known to be dual ERK5/bromodomain inhibitors, we analyzed the effect of ERK5 inhibition on genome-wide gene expression. Two cellular models with reported ERK5-regulated signaling were used: Pam_3CSK_4-stimulated HUVECs[23,38] and EGF-stimulated HeLa cells[20,26]. Cells were pre-incubated with DMSO vehicle, AX15836 (ERK5 inhibitor), AX15839 (dual ERK5/BRD inhibitor), or I-BET762 (BRD inhibitor), then stimulated with agonist. The HUVECs were confirmed to have been stimulated by TLR1/2 activation, and inhibited by AX15839 and I-BET762, by measurement of secreted IL-6 and IL-8 in sister wells (data not shown). The HeLa cells were confirmed to have been stimulated by EGF based on the appearance of phospho-ERK5 in sister wells (data not shown).

bioRxiv preprint doi: https://doi.org/10.1101/038513; this version posted February 2, 2016. The copyright holder for this preprint (which was not certified by peer review) is the author/funder. All rights reserved. No reuse allowed without permission.

RNA sequencing (RNA-Seq) of biological triplicates detected at least one transcript for 18925 genes in HUVEC samples and 17266 genes in HeLa samples. In both cell lines, samples treated with AX15836 showed very few genes to be differentially expressed (**Fig. 3a**). The total number of genes using the default cut-off (adjusted p-value ≤ 0.1) for MA plots was 7 in HUVEC samples and 2 in HeLa samples. Moreover, the observed maximal fold-changes in expression when compared to the DMSO control samples were modest: below 1.6 and 2 for HUVEC and HeLa samples, respectively (data not shown). Principal component analysis of all samples further confirmed the lack of differential gene expression in samples treated with the ERK5-only inhibitor AX15836 (**Fig. 3b**). Conversely, samples treated with the dual ERK5/BRD inhibitor AX15839 and those treated with the BRD inhibitor I-BET762 showed a large number of differentially expressed genes (**Fig. 3a**). The correlation of fold-changes in expression for all genes in samples treated with AX15839 and I-BET762 is shown in **Fig. 3c**. While there were some outliers, the majority of those genes showed comparable expression patterns in that they were expressed at either higher or lower levels in each of the treated samples when compared to controls. Likewise, the overlap of genes differentially expressed in these samples was significant for both cell types (**Fig. 3d**). In fact, all genes differentially expressed in one treatment were also differentially expressed in the other, albeit to a lesser extent or with a slightly higher adjusted p-value (data not shown).

bioRxiv preprint doi: https://doi.org/10.1101/038513; this version posted February 2, 2016. The copyright holder for this preprint (which was not certified by peer review) is the author/funder. All rights reserved. No reuse allowed without permission.

Figure 3. Differential gene expression in HUVEC and HeLa cells treated with AX15836, AX15839, and I-BET762.

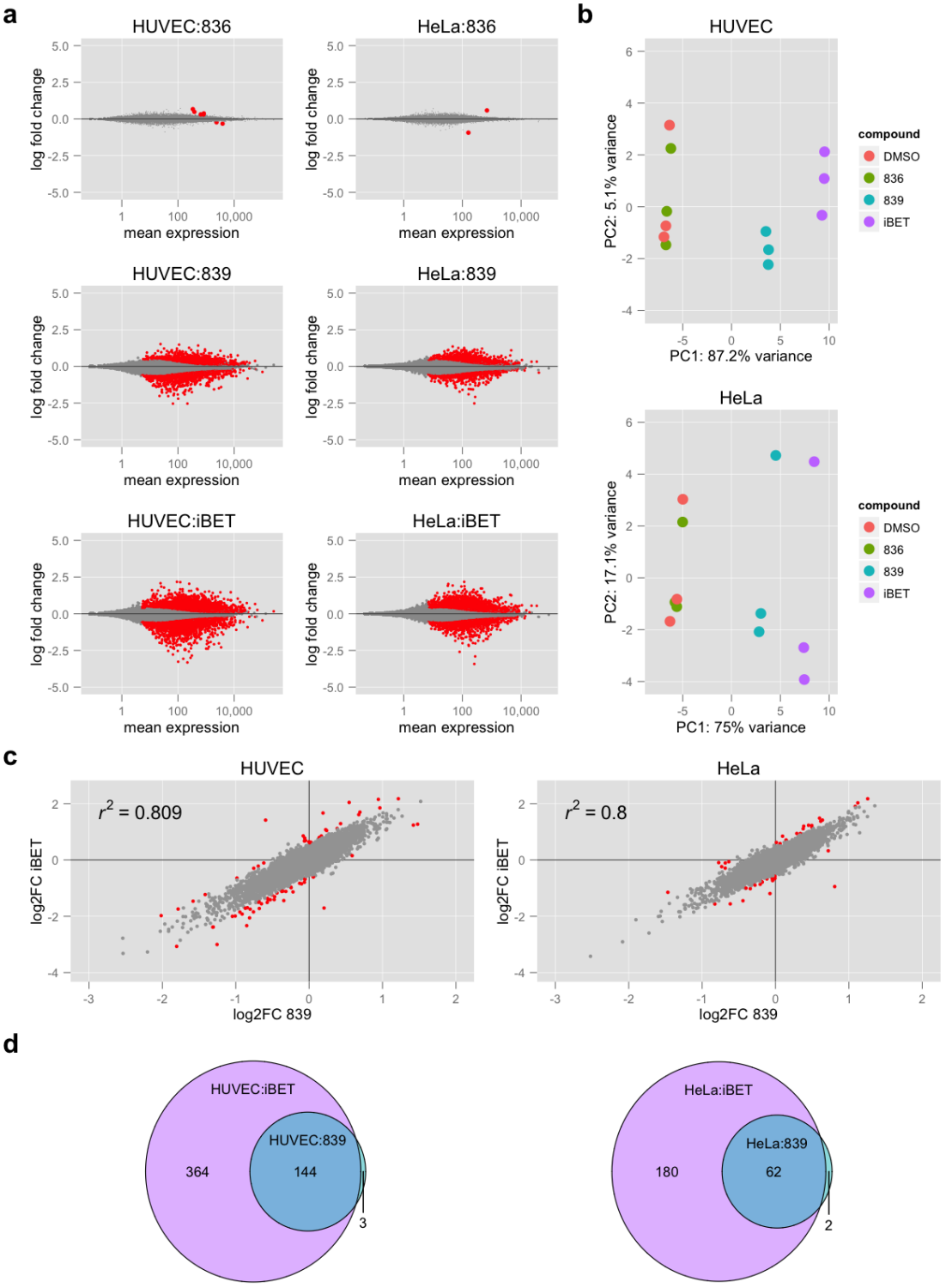

bioRxiv preprint doi: https://doi.org/10.1101/038513; this version posted February 2, 2016. The copyright holder for this preprint (which was not certified by peer review) is the author/funder. All rights reserved. No reuse allowed without permission.

(a) MA plots for HUVEC (left column) and HeLa cells (right column) treated with AX15836 (836, top row), AX15839 (839, middle row), and I-BET762 (iBET, bottom row). Differentially expressed genes with an adjusted p-value (DESeq2) of 0.1 or less are shown in red. **(b)** Principal component analysis of HUVEC (top) and HeLa cells (bottom) samples. **(c)** Correlation of gene expression profiles in HUVEC (left) and HeLa cells (right) treated with AX15839 and I-BET762. The log2-fold changes (log2FC) for compound-treated samples compared to the DMSO control samples are plotted for each gene. Outliers are highlighted in red and include those differentially expressed genes (at least a 1.5x fold-change and an adjusted p-value below 0.05 in one of the samples) with a residual outside of three times the standard deviation of all residuals. **(d)** Venn diagrams of differentially expressed genes (abs(log2FC) > 1 and adjusted p-value < 0.05) in HUVEC (left) and HeLa cells (right) treated with AX15839 and I-BET762.

bioRxiv preprint doi: https://doi.org/10.1101/038513; this version posted February 2, 2016. The copyright holder for this preprint (which was not certified by peer review) is the author/funder. All rights reserved. No reuse allowed without permission.

Looking at individual genes of interest, AX15839 and I-BET762 reduced Pam3CSK4-stimulated HUVEC gene expression of *IL6* (IL-6)(log2FC -0.72 and -1.32, respectively) and *CXCL8* (IL-8)(log2FC -0.73 and -1.42, respectively), consistent with our observation of decreased IL-6 and IL-8 protein in media of stimulated cells treated with the compounds. Gene expression of *SELE* (E-selectin) was also reduced by these compounds (log2FC -0.47 and -0.69, respectively). Additionally, both compounds with BRD inhibition (AX15839 and I-BET762) suppressed transcription of other genes involved in inflammation, such as *PTGS2* (COX-2), *CSF2* (GM-CSF), and *CCL2* (MCP-1), whereas inhibition of ERK5 kinase alone (AX15836) had no effect. Thus pharmacological inhibition of ERK5 kinase activity was not able to reduce inflammatory gene expression in endothelial cells, further supporting the concept that the previously-observed efficacy in first generation ERK5 inhibitors was due to an unrecognized inhibition of BRD/acetyl-lysine interaction.

EGF-mediated signaling in HeLa cells has been reported to increase transcripts for cytokines IL-6 and IL-8[39]. Our data from RNA-Seq indicated that BRD inhibition by AX15839 and I-BET762 strongly reduced the abundance of transcripts for *IL6* (log2FC -1.73 and -2.69, respectively) and *CXCL8* (log2FC -1.90 and -2.94, respectively). However, despite HeLa ERK5 phosphorylation being induced by EGF and inhibited by AX15836, we found no resulting impact on gene expression of solely inhibiting ERK5 kinase activity with AX15836.

bioRxiv preprint doi: https://doi.org/10.1101/038513; this version posted February 2, 2016. The copyright holder for this preprint (which was not certified by peer review) is the author/funder. All rights reserved. No reuse allowed without permission.

Discussion

ERK5 was proposed to have a role in inflammation due to the activity of the exemplar ERK5 inhibitor XMD8-92 and the corresponding effects of ERK5 silencing[23,38,40]. We have likewise observed similar reductions in inflammatory cytokine response using siRNA-mediated knockdown of ERK5 (data not shown) but upon further characterization of multiple ERK5 compounds, the similarities ended. Weiss and colleagues[41] described examples of the uncommon disconnect between results seen with gene knockdown versus pharmacological inhibition; although widely used together for verification, it was pointed out that they should actually not be expected to always align. With ERK5, pharmacological inhibition resulted in disparate biological effects (or more precisely, a lack of effect) as compared to deletion of the ERK5 protein, which adds to the understanding of the biology. While ERK5 kinase activity is thought to be important for direct phosphorylation of transcription factors and for regulating its own behavior by autophosphorylation, there is also evidence that ERK5-mediated transcription can occur independent of its kinase activity. Using specific antibodies against phosphorylated residues in the ERK5 C-terminus, Honda and colleagues[8] reported on the ability of growth factor-stimulated ERK1/2 to phosphorylate ERK5 at Thr732. This phosphosite was required for the ability of ERK5 to localize to the nucleus as well as to stimulate an ERK5-specific reporter gene. Interestingly, ERK1/2 activity on a kinase-inactive ERK5 mutant (K83M) could likewise do the same, suggesting that under conditions such as growth factor stimulation, ERK5 kinase activity was not necessary for ERK5-mediated effects. Another study demonstrating alternative regulation of ERK5 phosphorylation supports the ability of ERK5 to function aside from its kinase activity: using a kinase-inactive ERK5 mutant (K83S, K84L) or just the C-terminal domain, Diez-Rodriguez and Pandiella[6] found that ERK5 could be phosphorylated on C-terminal

bioRxiv preprint doi: https://doi.org/10.1101/038513; this version posted February 2, 2016. The copyright holder for this preprint (which was not certified by peer review) is the author/funder. All rights reserved. No reuse allowed without permission.

residues during mitosis to affect transcriptional activity, without requiring kinase activity. Thus it seems clear that ERK5 can regulate biological functions independent of its kinase activity.

As it turns out, XMD8-92 and other first generation ERK5 inhibitors exhibited potent BRD inhibition. Numerous kinase inhibitors, many quite selective among the kinases, have recently been shown to inhibit BRD/acetyl-lysine binding. Martin and colleagues discovered that the cyclin-dependent kinase (CDK) inhibitor dinaciclib could bind to BRDT(1) and hypothesized that other hinge-binding kinase inhibitors would also bind to bromodomains[28]. The group followed with an ambitious co-crystallization screening approach of BRD4(1) against a library of over 580 diverse kinase inhibitors, and indeed were able to identify 14 BRD-inhibiting compounds[29]. Likewise, Ciceri and colleagues used a biochemical approach to screen a library of 628 kinase-selective inhibitors (including > 200 clinical compounds) for BRD4(1) inhibition and found nine that strongly inhibited the binding of a poly-acetylated histone H4 peptide[30]. These studies demonstrate that kinases and bromodomains can share a high degree of pharmacophore similarity and call for an increased awareness for possible epigenetic modifications by seemingly specific kinase inhibitors.

Inhibition of the BET family of bromodomain-containing proteins has been shown to effectively modulate inflammation, including cytokine- or toll-like receptor-stimulated inflammatory responses[33,42–44]. While we did not find any anti-inflammatory effect using ERK5-specific inhibitors that lack potent BRD inhibition, we did observe efficacy that can be attributed to the BRD inhibition in dual ERK/BRD inhibitors. Preliminary experiments also found no anti-proliferative effects of our ERK5-only inhibitors, suggesting that recent reports supporting ERK5 as a drug target for cancer should be subject to re-evaluation. Nonetheless, compounds such as

bioRxiv preprint doi: https://doi.org/10.1101/038513; this version posted February 2, 2016. The copyright holder for this preprint (which was not certified by peer review) is the author/funder. All rights reserved. No reuse allowed without permission.

AX15836 represent a new generation of specific ERK5 inhibitors that should prove to be valuable tools for delineating the complex biology of ERK5.

bioRxiv preprint doi: https://doi.org/10.1101/038513; this version posted February 2, 2016. The copyright holder for this preprint (which was not certified by peer review) is the author/funder. All rights reserved. No reuse allowed without permission.

Online Methods

Materials

TLR2 agonist peptide Pam_3CSK_4 was purchased from Enzo Life Sciences (Farmingdale, NY). Recombinant human epidermal growth factor (EGF) and IL-17A were from EMD Millipore (Billerica, MA) and eBioscience (San Diego, CA), respectively. Antibodies against ERK5, β-actin, GAPDH, and DyLight 680 and 800 conjugated secondary antibodies were purchased from Cell Signaling Technology (Danvers, MA). Human IgG, fluorescein-conjugated anti-E-selectin (Clone BBIG-E5) and anti-IgG_1 isotype control antibodies were obtained from R&D Systems/Bio-Techne (Minneapolis, MN). I-BET762 and JQ1 were purchased from Selleck Chemicals (Houston, TX). XMD8-92 was purchased from Tocris/Bio-Techne as well as synthesized in house as described[19]. Commercial compound structures and batch purities (≥ 99%) were reported by the manufacturers using standard analytical methods (HPLC and NMR).

For compound synthesis, Compound **1** was purchased from Shanghai IS Chemical Technology. Proton nuclear magnetic resonance (^{1}H NMR) spectra were recorded on a Bruker 400 MHz NMR spectrometer in deuterated solvents using the residual ^{1}H solvent peak as the internal standard. LC/MS (ES) analysis was performed with an Agilent 1260 Infinity Series LC/MSD using ChemStation software equipped with a C_{18} reverse phase column (Phenomenex Kinetex 5 m XB-C18 50 x 2.10 mm column, or Agilent Poreshell 120 EC-C18 3.0 x 50 mm column), or Agilent 1100 Series LC/MSD using ChemStation software equipped with a C_{18} reverse phase column (Onyx, monolithic C18 column, 50 x 2.0 mm; Phenomenex; Torrance, CA), and using a binary system of water and acetonitrile with 0.1% trifluoroacetic acid as a modifier. Flash silica gel column chromatography was carried out on a CombiFlash R_f system

bioRxiv preprint doi: https://doi.org/10.1101/038513; this version posted February 2, 2016. The copyright holder for this preprint (which was not certified by peer review) is the author/funder. All rights reserved. No reuse allowed without permission.

(by Teledyne ISCO) or a Biotage SP-4 automated purification system using pre-packed silica gel cartridges. HPLC purification was performed by using an Agilent 1200 Series with a C_{18} reverse phase column (Luna 5 u C18 (2) 100A, 150 x 21.2 mm, 5 micron; Phenomenex; Torrance, CA) and using a binary system of water and acetonitrile with 0.1% acetic acid as a modifier.

Synthetic Protocols

Scheme for the synthesis of AX15836

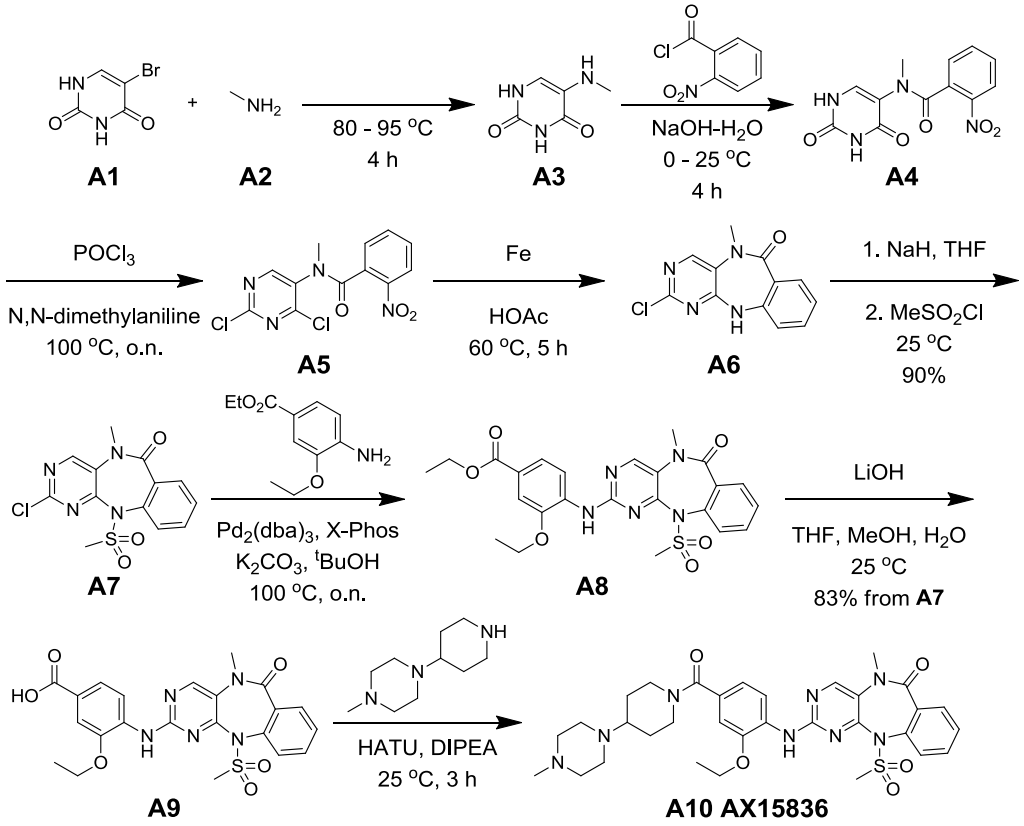

bioRxiv preprint doi: https://doi.org/10.1101/038513; this version posted February 2, 2016. The copyright holder for this preprint (which was not certified by peer review) is the author/funder. All rights reserved. No reuse allowed without permission.

5-(Methylamino)pyrimidine-2,4(1H,3H)-dione (A3). To a 500 mL 3-neck round bottom flask filled with a condenser, 5-bromopyrimidine-2,4(1H,3H)-dione (**A1**, 20 g, 0.10 mol) and methanamine (**A2**, 40% aqueous solution, 160 mL, 1.85 mol) were added. The reaction mixture was stirred and heated at 80 ^{o}C for 3.5 hours. At 25 ^{o}C, the reaction mixture was acidified to pH ~ 4.5 with diluted HCl aqueous solution. The generated light yellow precipitates were filtered and washed with water, then dried in vacuo to provide **A3** (10.46 g, 70%) as a light yellow solid. ESMS found *m/z* 142.1 ([M + H^+], $C_5H_7N_3O_2$ requires 141.0538).

N-(2,4-Dioxo-1,2,3,4-tetrahydropyrimidin-5-yl)-N-methyl-2-nitrobenzamide (A4). To a solution of **A3** (10.46 gram, 74.1 mmol) in THF (40 mL) was added NaOH aqueous solution (2.5 N, 100 mL, 250 mmol) at 0 ^{o}C. Then 2-nitrobenzoyl chloride (12.8 mL, 96.8 mmol) was added slowly. The generated clear brown solution was stirred at 0 ^{o}C for 40 minutes then at room temperature for 4.5 h. The reaction mixture was acidified by diluted HCl aqueous solution and stored for 3 days. The generated light yellow solid was filtered and the cake was washed with water, then dried in vacuo to provide **A4** (13.47 g, 63%) as light yellow solid. ESMS found *m/z* 291.0 ([M + H^+], $C_{12}H_{10}N_4O_5$ requires 290.0651), 313.1 [M + Na^+],.

N-(2,4-Dichloropyrimidin-5-yl)-N-methyl-2-nitrobenzamide (A5). A solution of **A4** (7.96 g, 27.4 mmol) and N,N-dimethylaniline (3 mL, 23.7 mmol) in phosphorus oxychloride ($POCl_3$, 135 mL, 1.45 mol) was heated at 100 ^{o}C overnight. The solvent was removed by rotavapor and the residue was dried in vacuo to provide the crude product **A5**, which was used for next step reaction without further purification. ESMS found *m/z* 327.0, 329.0 ([M + H^+], $C_{12}H_8C_{l2}N_4O_3$ requires 325.9973, 327.9944).

bioRxiv preprint doi: https://doi.org/10.1101/038513; this version posted February 2, 2016. The copyright holder for this preprint (which was not certified by peer review) is the author/funder. All rights reserved. No reuse allowed without permission.

2-Chloro-5-methyl-5H-benzo[e]pyrimido[5,4-b][1,4]diazepin-6(11H)-one (A6). The crude **A5** (~ 27.4 mmol, from last step) was dissolved in acetic acid (100 mL), then iron (9.1 g, 163 mmol) was added at 25 ^{o}C with rigorous stirring. The mixture was heated at 60 ^{o}C for 5 h. Water (100 mL) and ethanol (10 mL) were added and the reaction mixture was stirred for additional 30 minutes. The precipitates were filtered and extracted between ethyl acetate and water. The combined EtOAc phase was dried over sodium sulfate and then concentrated to produce the crude **A6** (3.25 g, 46% for two steps). ^{1}H NMR (400 MHz, $CDCl_3$) δ 8.23 (s, 1H), 7.98 (dd, J = 1.5, 8.0, 1H), 7.45 – 7.37 (m, 1H), 7.17 – 7.09 (m, 1H), 6.82 (dd, J = 0.9, 8.1, 1H), 6.71 (s, 1H), 3.51 (s, 3H); ESMS found *m/z* 261.1 ([M + H^{+}], $C_{12}H_9ClN_4O$ requires 260.0465).

2-Chloro-5-methyl-11-(methylsulfonyl)-5H-benzo[e]pyrimido[5,4-b][1,4]diazepin-6(11H)-one (A7). NaH (60%, 160.0 mg, 4.00 mmol) was added to a solution of **A6** (521.4 mg, 2.00 mmol) in THF (20.0 mL) at 0 ^{o}C. The generated orange suspension was stirred at 25 ^{o}C for 30 min, then $MeSO_2Cl$ (310.0 μL, 4.00 mmol) was added and the mixture was stirred at 25 ^{o}C for 1 h. The reaction was quenched and diluted with H_2O. The aqueous phase was extracted with EtOAc. The combined EtOAc phase was washed with sat. $NaHCO_3$ and sat. NaCl aqueous solution, then dried over Na_2SO_4. The dried organic phase was filtered and concentrated by rotavapor. The residue was washed with hexane, and the gum was dried in vacuo to provide the crude **A7** as a light yellow solid, which was used for next step reaction without further purification. ^{1}H NMR (400 MHz, DMSO-d_6) δ 9.07 (s, 1H), 7.82 (dd, J = 1.2, 7.5, 1H), 7.74 – 7.64 (m, 2H), 7.54 (ddd, J = 2.1, 6.5, 7.8, 1H), 3.79 (s, 3H), 3.56 (s, 3H); ESMS found *m/z* 339.0 ([M + H^{+}], $C_{13}H_{11}ClN_4O_3S$ requires 338.0240).

bioRxiv preprint doi: https://doi.org/10.1101/038513; this version posted February 2, 2016. The copyright holder for this preprint (which was not certified by peer review) is the author/funder. All rights reserved. No reuse allowed without permission.

Ethyl 3-ethoxy-4-(5-methyl-11-(methylsulfonyl)-6-oxo-6,11-dihydro-5H-benzo[e]pyrimido [5,4-b][1,4]diazepin-2-ylamino)benzoate (A8). A mixture of crude **A7** (367 mg, ~ 92% purity, ~ 1.00 mmol), ethyl 4-amino-3-ethoxybenzoate (251.1 mg, 1.20 mmol), X-Phos (42.0 mg, 0.088 mmol), and K_2CO_3 (829.3 mg, 6.00 mmol) in ^{t}BuOH (10.0 mL) was bubbled with N_2 for 20 sec. $Pd_2(dba)_3$ (54.9 mg, 0.060 mmol) was added and the mixture was bubbled with N_2 for additional 20 sec. The mixture was then heated at 100 ^{o}C under N_2 overnight. The reaction mixture was diluted with hexane-EtOAc solution (10:3). The precipitates were filtered and washed with hexane-EtOAc solution (10:3). The combined filtrate was concentrated in vacuo to provide the crude **A8** as an orange solid, which was used for next step reaction without further purification. ESMS found *m/z* 512.1 ([M + H$^+$], $C_{24}H_{25}N_5O_6S$ requires 511.1526).

3-Ethoxy-4-(5-methyl-11-(methylsulfonyl)-6-oxo-6,11-dihydro-5H-benzo[e] pyrimido[5,4-b][1,4]diazepin-2-ylamino)benzoic acid (A9). A solution of the crude **A8** (699.0 mg, ~ 73.2%, ~ 1.000 mmol) in THF (6.05.4 mL), MeOH (2.0 mL), and H_2O (2.0 mL) was treated with LiOH hydrate (62.9 mg, 1.50 mmol) at 25 ^{o}C overnight. The reaction mixture was concentrated by rotavapor. The residue was diluted with DCM. The DCM phase was extracted with 1 N NaOH aqueous solution. The combined aqueous phase was washed with additional DCM. Then the aqueous phase was acidified with 1 N HCl aqueous solution. The generated precipitates were stirred for 10 min, filtered and washed with H_2O, then dried in vacuo to provide **A9** (389.3 mg, 81% for 3 steps) as a tan solid. ^{1}H NMR (400 MHz, DMSO-d$_6$) δ 12.70 (br s, 1H), 9.02 (s, 1H), 8.79 (s, 1H), 8.00 (d, J = 8.3, 1H), 7.78 (d, J = 7.8, 1H), 7.65 (s, 1H), 7.63 – 7.55 (m, 2H), 7.53

bioRxiv preprint doi: https://doi.org/10.1101/038513; this version posted February 2, 2016. The copyright holder for this preprint (which was not certified by peer review) is the author/funder. All rights reserved. No reuse allowed without permission.

(s, 1H), 7.49 (s, 1H), 4.16 (m, 2H), 3.80 (s, 3H), 3.51 (s, 3H), 1.32 (t, *J* = 6.9, 3H); ESMS found *m/z* 484.2 ([M + H^+], $C_{22}H_{21}N_5O_6S$ requires 483.1213).

2-(2-Ethoxy-4-(4-(4-methylpiperazin-1-yl)piperidine-1-carbonyl)phenylamino)-5-methyl-11-(methylsulfonyl)-5H-benzo[e]pyrimido[5,4-b][1,4]diazepin-6(11H)-one (A10, AX15836). HATU (356.5 mg, 0.938 mmol) was added to a solution of **A9** (377.8 mg, 0.781 mmol), 1-methyl-4-(piperidin-4-yl)piperazine (171.9 mg, 0.938 mmol) and DIPEA (408.0 μL, 2.34 mmol) in DMF (3.9 mL) at 25 ^{o}C. The mixture was stirred at 25 ^{o}C for 3 h. The reaction mixture was dried in vacuo. The residue was purified by HPLC to provide the acetic acid salt of **A10** (**AX15836**, 140 mg, 98% purity, 28%) as a white solid. ^{1}H NMR (400 MHz, DMSO-d_6) δ 9.02 (s, 1H), 8.73 (s, 1H), 7.80 – 7.75 (m, 1H), 7.72 (d, *J* = 8.0, 1H), 7.67 – 7.57 (m, 2H), 7.48 (dd, *J* = 5.1, 11.1, 1H), 7.03 (d, *J* = 1.6, 1H), 7.00 – 6.93 (m, 1H), 4.58 – 4.26 (m, 1H), 4.16 – 4.01 (m, 2H), 3.74 (s, 3H), 3.72 – 3.55 (m, 1H), 3.49 (s, 3H), 3.15 – 2.88 (m, 1H), 2.86 – 2.63 (m, 1H), 2.55 (d, *J* = 0.5, 3H), 2.50 (m, 5H), 2.29 (m, 3H), 2.13 (s, 3H), 1.79 (m, 2H), 1.37 (m, 2H), 1.24 (t, *J* = 6.9, 3H). ^{13}C NMR (400 MHz, DMSO-d_6) δ 169.01, 166.02, 157.48, 156.06, 155.74, 150.69, 140.68, 133.32, 132.97, 132.20, 130.63, 129.05, 128.70, 125.74, 124.63, 123.18, 119.12, 111.33, 64.38, 61.31, 55.60, 48.99, 46.23, 45.42, 40.83, 37.36, 24.44, 14.91; ESMS found *m/z* 649.3 ([M + H^+], $C_{32}H_{40}N_8O_5S$ requires 648.2842).

Scheme for the synthesis of AX15839 & AX15910

bioRxiv preprint doi: https://doi.org/10.1101/038513; this version posted February 2, 2016. The copyright holder for this preprint (which was not certified by peer review) is the author/funder. All rights reserved. No reuse allowed without permission.

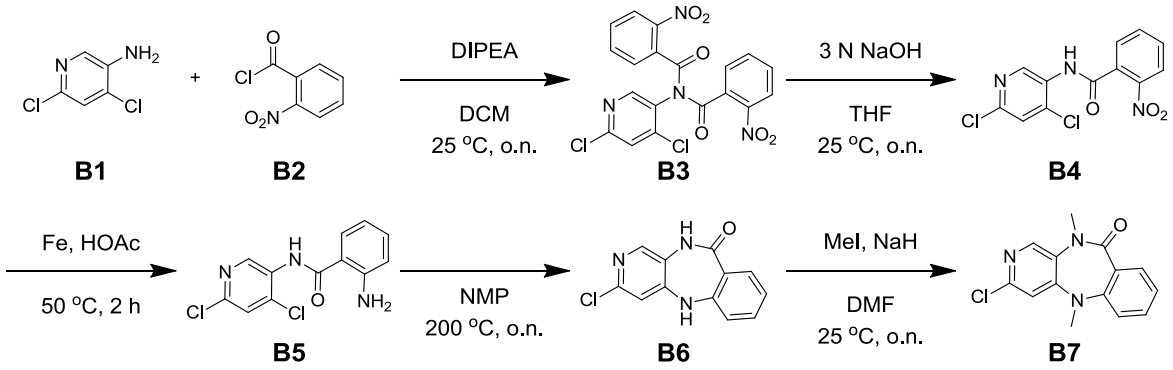

N-(4, 6-Dichloropyridin-3-yl)-2-nitro-N-(2-nitrobenzoyl)benzamide (B3). 2-Nitrobenzoyl chloride (**B2**, 11.10 mL, 84.0 mmol) was added slowly to a solution of 5-amino-2, 4-dichloropyridine (**B1**, 6.520 g, 40.0 mmol) and DIPEA (27.9 mL, 160 mmol) in DCM (100 mL) at 0 ^{o}C under N_2. The mixture was then stirred at 25 ^{o}C for 1.5 h. The reaction mixture was concentrated by rotavapor. And the residue **B3** (brown syrup) was used for the next step without further purification.

A small amount of the reaction mixture was diluted with DCM, and washed with H_2O, sat. $NaHCO_3$ aqueous solution and sat. NaCl aqueous solution, then dried over Na_2SO_4. The dried organic phase was filtered and concentrated. The residue was rinsed with small amount of DCM and the remaining precipitates were dried in vacuo to provide **B3** as a white solid. ^{1}H NMR (400 MHz, DMSO-d6) δ 8.63 (s, 1H), 8.24 (d, J = 8.3, 2H), 8.08 (d, J = 1.0, 1H), 7.97 – 7.80 (m, 4H), 7.75 (t, J = 7.8, 2H); ESMS found *m/z* 461.0 ([M + H^{+}], $C_{19}H_{10}Cl_2N_4O_6$ requires 459.9977), 483.0 [M + Na^{+}].

N-(4, 6-Dichloropyridin-3-yl)-2-nitrobenzamide (B4). A suspension of above crude **B3** (~ 40.0 mmol) in THF (90 mL) and NaOH aqueous solution (~ 3.5 N, 72 mL, ~ 252 mmol) was stirred

bioRxiv preprint doi: https://doi.org/10.1101/038513; this version posted February 2, 2016. The copyright holder for this preprint (which was not certified by peer review) is the author/funder. All rights reserved. No reuse allowed without permission.

rigorously at 25 ^{o}C overnight. The reaction mixture was diluted with sat. NaCl aqueous solution. The aqueous phase was extracted with EtOAc. The combined organic phase was washed with sat. $NaHCO_3$ and sat. NaCl solution, then dried over $NaSO_4$. Filtration and concentration in vacuo provided **B4** (11.24 g, 90% for two steps) as a pale white solid. ^{1}H NMR (400 MHz, $CDCl_3$) δ 9.42 (br s, 1H), 8.19 (dd, J = 1.0, 8.2, 1H), 7.74 (m, 4H), 7.45 (s, 1H); ESMS found *m/z* 312.0, 314.0 ([M + H^+], $C_{12}H_7Cl_2N_3O_3$ requires 310.9864, 312.9835), 334.0, 336.0 [M + Na^+].

2-Amino-N-(4, 6-dichloropyridin-3-yl)benzamide (B5). A suspension of **B4** (12.48 g, 35.80 mmol) and Fe (4.47 g, 80.0 mmol) in HOAc (80 mL) was heated at 50 ^{o}C with rigorous stirring under N_2 for 2 h. Additional Fe (1.12 g, 10 mmol) was added twice during 2 h. The reaction mixture was stirred at 50 ^{o}C for additional 1 h. At 25 ^{o}C, the extra Fe was removed with a magnetic bar. The reaction mixture was quenched with 1 N NaOH aqueous solution and the aqueous solution was saturated with NaCl. The product was extracted by EtOAc (multiple times and monitored by LCMS). The combined EtOAc phase was washed with sat. $NaHCO_3$ solution and sat. NaCl solution, then dried over Na_2SO_4. Filtration and concentration in vacuo to provide **B5** (10.26 g, 91%) as a pale white solid. ^{1}H NMR (400 MHz, DMSO-d6) δ 10.07 (br s, 1H), 8.56 (s, 1H), 7.94 (t, J = 1.6, 1H), 7.74 (dd, J = 1.4, 8.0, 1H), 7.25 (ddd, J = 1.5, 7.1, 8.4, 1H), 6.78 (dd, J = 0.9, 8.3, 1H), 6.67 – 6.58 (m, 1H), 6.53 (br s, 2H); ESMS found *m/z* 282.1, 284.0 ([M + H^+], $C_{12}H_9Cl_2N_3O$ requires 281.0123, 283.0093), 304.0, 306.0 [M + Na^+].

bioRxiv preprint doi: https://doi.org/10.1101/038513; this version posted February 2, 2016. The copyright holder for this preprint (which was not certified by peer review) is the author/funder. All rights reserved. No reuse allowed without permission.

3-Chloro-5H-benzo[e]pyrido[3,4-b][1,4]diazepin-10(11H)-one (B6). A suspension of **B5** (10.263 g, 36.38 mmol) in NMP (80.0 mL) was heated at 200 ^{o}C under N_2 for 4 h. At 25 ^{o}C, a diluted HCl aqueous solution (0.33 N, 240 mL) was added. The generated suspension was stirred at 25 ^{o}C for 1 h. The precipitates were filtered and washed with H_2O, then dried in vacuo to provide **B6** (8.623 g, 96%) as a yellow solid. ^{1}H NMR (400 MHz, DMSO-d6) δ 10.05 (s, 1H), 8.76 (s, 1H), 7.85 (s, 1H), 7.80 – 7.68 (m, 1H), 7.47 – 7.32 (m, 1H), 6.96 (m, 3H); ESMS found *m/z* 246.1 ([M + H^{+}], $C_{12}H_8ClN_3O$ requires 245.0356), 268.0 [M + Na^{+}].

3-Chloro-5,11-dimethyl-5H-benzo[e]pyrido[3,4-b][1,4]diazepin-10(11H)-one (B7). NaH (60%, 2.15 g, 53.9 mmol) was added portionwise to a suspension of **B6** (5.513 g, 22.4 mmol) and MeI (3.36 mL, 53.9 mmol) in anhydrous DMF (67.3 mL) at 0 ^{o}C under N_2. The reaction mixture was then stirred at 25 ^{o}C under N_2 overnight. At 0 ^{o}C, the diluted HCl aqueous solution (0.25 N) was added slowly to the generated suspension reaction mixture. The mixture was stirred at 25 ^{o}C for 1 h. Hexanes was added and the mixture was stirred at 25 ^{o}C for additional 1 h. The generated precipitates were filtered and washed with H_2O, then dried in vacuo to provide **B7** (5.145 g, 84%) as yellow solid. ^{1}H NMR (400 MHz, DMSO-d6) δ 8.36 (s, 1H), 7.65 (dd, J = 1.7, 7.7, 1H), 7.55 – 7.44 (m, 1H), 7.34 (s, 1H), 7.23 – 7.11 (m, 2H), 3.45 (s, 3H), 3.31 (s, 3H); ESMS found *m/z* 274.1 ([M + H^{+}], $C_{14}H_{12}ClN_3O$ requires 273.0669), 296.1 [M + Na^{+}].

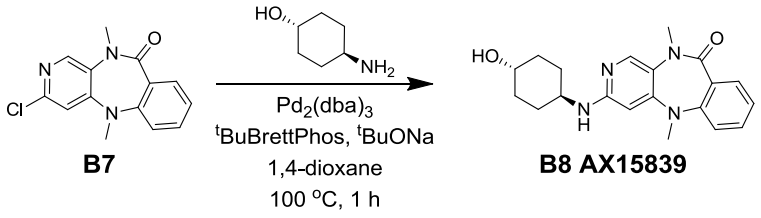

bioRxiv preprint doi: https://doi.org/10.1101/038513; this version posted February 2, 2016. The copyright holder for this preprint (which was not certified by peer review) is the author/funder. All rights reserved. No reuse allowed without permission.

3-((1r,4r)-4-Hydroxycyclohexylamino)-5,11-dimethyl-5H-benzo[e]pyrido[3,4-b][1,4]diazepin-10(11H)-one (B8, AX15839). A mixture of **B7** (4.13 g, 15.1 mmol), *trans*-4-aminocyclohexanol (2.09 g, 18.1 mmol), $Pd_2(dba)_3$ (691 mg, 0.755 mmol), ^{t}BuBrettPhos (732 mg, 1.51 mmol), and ^{t}BuONa (5.08 g, 52.9 mmol) in 1,4-dioxane (150 mL) was bubbled with N_2 at 25 ^{o}C then stirred at 100 ^{o}C for 1 h. After cooling to room temperature, the reaction mixture was filtered *through* a *pad* of *Celite* pad, then the solvent was removed under reduced pressure. After the purification by silica gel column chromatography (Biotage Ultra 100 g, toluene to 15% ethanol-toluene), the residue was suspended with ethyl acetate. The precipitate was collected by filtration and then dried in vacuo to afford **B8** (2.30 g, 95% purity, 43%) as a pale yellow solid. ^{1}H NMR (400 MHz, DMSO-d_6) δ 1.11-1.20 (4H, m), 1.80-1.88 (4H, s), 3.17 (3H, s), 3.37 (3H, s), 3.38 (1H, brs), 3.57-3.58 (1H, m), 4.50 (1H, d, J = 4.4 Hz), 6.18 (1H, s), 6.34 (1H, d, J = 8.0 Hz), 7.11 (1H, t, J = 8.0 Hz), 7.17 (1H, d, J = 8.0 Hz), 7.45 (1H, t, J = 8.0 Hz), 7.60 (1H, d, J = 8.0 Hz), 7.92 (1H, s); ^{13}C NMR (101 MHz, DMSO-d6) δ 167.95, 157.12, 156.33, 151.78, 142.88, 132.53, 131.82, 127.50, 123.79, 123.51, 117.31, 96.42, 68.87, 49.08, 38.14, 36.75, 34.50, 34.46, 31.05, 30.96; HRESIMS found *m/z* 353.19729 ([M+H$^+$], $C_{20}H_{24}N_4O_2$ requires 352.1899).

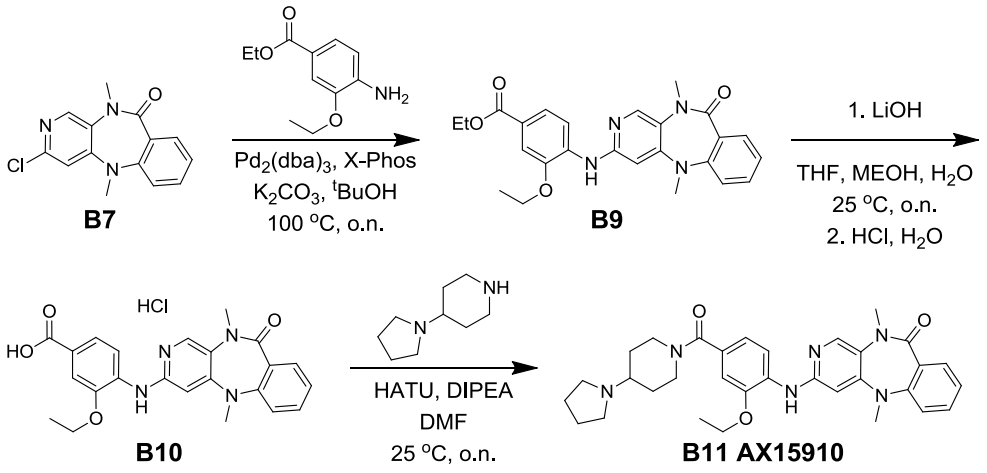

bioRxiv preprint doi: https://doi.org/10.1101/038513; this version posted February 2, 2016. The copyright holder for this preprint (which was not certified by peer review) is the author/funder. All rights reserved. No reuse allowed without permission.

Ethyl 4-(5,11-dimethyl-10-oxo-10,11-dihydro-5H-benzo[e]pyrido[3,4-b][1,4]diazepin-3-ylamino)-3-ethoxybenzoate (B9). A mixture of **B7** (4.927 g, 18.0 mmol), ethyl 4-amino-3-ethoxybenzoate (4.520 g, 21.6 mmol), X-Phos (755.1 mg, 1.58 mmol), and K_2CO_3 (14.93 g, 108.0 mmol) in ^{t}BuOH (90 mL) was bubbled with N_2 for 30 sec. $Pd_2(dba)_3$ (494.5 mg, 0.540 mmol) was added and the mixture was bubbled with N_2 for additional 1 minute. The suspension was then heated at 100 ^{o}C (flushed with condenser) under N_2 for 23 h. The reaction mixture was diluted with EtOAc at 25 ^{o}C. The suspension was filtered through a premade Celite filter column and the precipitates were washed with EtOAc. The filtrate was washed with 0.5 N HCl aqueous solution and sat. NaCl aqueous solution, then dried over Na_2SO_4. The organic solution was filtrated and concentrated by rotavapor. The residue was diluted with CH_3CN. The small amount of insoluble yellow solid was filtered and the CH_3CN filtrate was concentrated and dried in vacuo to provide the crude **B9** as a yellow solid, which was used for next step reaction without further purification. ESMS found *m/z* 447.2 ([M+H$^+$], $C_{25}H_{26}N_4O_4$ requires 446.1954), 469.1 [M + Na$^+$].

4-(5,11-Dimethyl-10-oxo-10,11-dihydro-5H-benzo[e]pyrido[3,4-b][1,4]diazepin-3-ylamino)-3-ethoxybenzoic acid (B10). The crude **B9** (~ 78.5% pure, 10.00 g, ~ 17.6 mmol) was dissolved in THF (52.7 mL), MeOH (17.6 mL) and H_2O (17.6 mL). LiOH monohydrate (2.066 g, 49.2 mmol) was added and the mixture was stirred at 25 ^{o}C for 4 h. Additional LiOH monohydrate (1.033 g, 24.6 mmol) and H_2O (10 mL) were added and the mixture was stirred at 25 ^{o}C for additional 1.5 h. The reaction mixture was concentrated by rotavapor. The residue was diluted with 0.5 N NaOH aqueous solution. The basic aqueous phase was washed with ether then acidified with 3 N HCl solution. The generated precipitates were filtered and washed with H_2O,

bioRxiv preprint doi: https://doi.org/10.1101/038513; this version posted February 2, 2016. The copyright holder for this preprint (which was not certified by peer review) is the author/funder. All rights reserved. No reuse allowed without permission.

and rinsed with small amount of EtOAc, then dried in vacuo to provide **B10** (6.071 g, 81% for two steps) as a tan solid. ^{1}H NMR (400 MHz, DMSO-d6) δ 9.65 – 9.27 (br s, 1H), 8.14 (s, 1H), 8.00 (br s, 1H), 7.68 (dd, *J* = 1.7, 7.7, 1H), 7.64 – 7.44 (m, 3H), 7.29 (d, *J* = 8.1, 1H), 7.20 (t, *J* = 7.5, 1H), 7.05 (s, 1H), 4.17 (q, *J* = 7.0, 2H), 3.45 (s, 3H), 3.33 (s, 3H), 1.33 (t, *J* = 6.9, 3H); ESMS *m/z*: 419.1 [M + H^{+}]. ESMS found *m/z* 419.1 ([M+H^{+}], $C_{23}H_{22}N_4O_4$ requires 418.1641).

3-(2-Ethoxy-4-(4-(pyrrolidin-1-yl)piperidine-1-carbonyl)phenylamino)-5,11-dimethyl-5H-benzo[e]pyrido[3,4-b][1,4]diazepin-10(11H)-one (B11, AX15910). To a solution of **B10** (2.40 g, 5.74 mmol) and 4-pyrrolidin-1-ylpiperidine (1.062 g, 6.88 mmol) in DMF (30 mL) were add DIPEA (4.00 mL, 22.9 mmol) and HATU (3.053 g, 8.03 mmol) at 25 ^{o}C. The reaction mixture was stirred at 25 ^{o}C for 2 h and then concentrated by a lyophilizer. Water was added to the residue and the mixture was stirred at 25 ^{o}C for 30 minutes. The generated precipitates were filtered and purified by prep HPLC. Lyophilization of the pure product fractions provided **B11** (**AX15910**, 2.15 g, > 95% purity, 68%) as a white powder. ^{1}H NMR (400 MHz, $CDCl_3$) δ 8.11 – 8.01 (m, 2H), 7.83 (dd, *J* = 1.7, 7.7, 1H), 7.45 – 7.36 (m, 1H), 7.12 (dd, *J* = 3.1, 10.7, 2H), 7.06 – 6.96 (m, 3H), 6.53 (s, 1H), 4.13 (q, *J* = 7.0, 2H), 3.57 (s, 3H), 3.31 (s, 3H), 2.93 (s, 2H), 2.75 (s, 4H), 2.47 (s, 1H), 2.02 (s, 1H), 2.02 – 1.92 (m, 2H), 1.87 (s, 4H), 1.65 (s, 2H), 1.47 (t, *J* = 7.0, 3H); ^{13}C NMR (101 MHz, DMSO-d6) δ 169.47, 167.90, 156.31, 153.96, 151.73, 147.11, 142.17, 132.81, 132.09, 132.00, 128.59, 127.17, 126.78, 123.70, 119.78, 117.90, 117.48, 111.03, 100.84, 64.48, 61.20, 51.27, 40.38, 38.16, 23.38, 17.20, 15.06; ESMS found *m/z* 555.3 ([M+H^{+}], $C_{32}H_{38}N_6O_3$ requires 554.3005), 1131.6 [2M + Na^{+}].

Scheme of synthesis of AX15892

bioRxiv preprint doi: https://doi.org/10.1101/038513; this version posted February 2, 2016. The copyright holder for this preprint (which was not certified by peer review) is the author/funder. All rights reserved. No reuse allowed without permission.

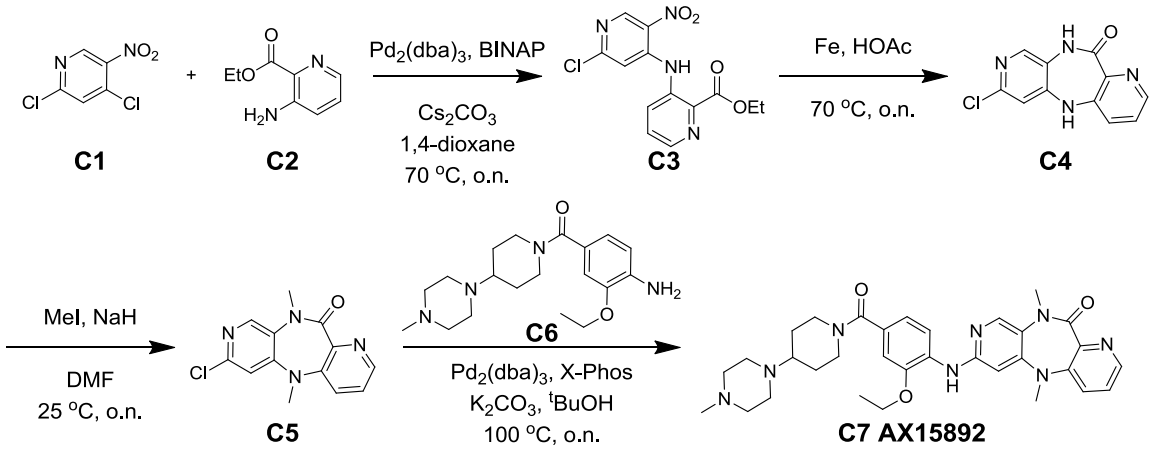

Ethyl 3-[(2-chloro-5-nitro-4-pyridyl)amino]pyridine-2-carboxylate (C3). A mixture of 2,4-dichloro-5-nitro-pyridine (**C1**, 1.0 g, 5.2 mmol), ethyl 3-aminopyridine-2-carboxylate (**C2**, 0.86 g, 5.2 mmol), Cs_2CO_3 (3.38 g, 10.4 mmol) and BINAP (0.19 g, 0.31 mmol) in anhydrous 1,4-dioxane (133 mL) was degassed with N_2 at 25 ^oC, then $Pd_2(dba)_3$ (0.19 g, 0.21 mmol) was added. The mixture was degassed again and heated at 70 °C overnight. The reaction was filtered through Celite and washed with DCM. The filtrate was concentrated, and the resulting residue was purified by silica gel flash chromatography using EtOAc / Hexane as eluent solution. The product containing fractions were concentrated to provide **C3** (0.653 g, 39 %) as a yellow solid. ^1H NMR (400 MHz, $CDCl_3$) δ 11.48 (s, 1H), 9.18 (s, 1H), 8.71 – 8.60 (m, 1H), 8.02 (d, J = 8.4, 1H), 7.64 (dd, J = 4.5, 8.4, 1H), 7.27 (s, 1H), 4.58 (q, J = 7.1, 2H), 1.50 (t, J = 7.1, 3H); ESMS found *m/z* 323.1 ([M + H^+], $C_{13}H_{11}ClN_4O_4$ requires 322.0469).

7-Chloro-5H-dipyrido[3,4-b:3',2'-e][1,4]diazepin-11(10H)-one (C4). To a solution of **C3** (653 mg, 2.02 mmol) in AcOH (10 mL) was added Fe powder (560 mg, 10.1 mmol) at 25 ^oC. The mixture was then heated at 70 °C overnight. The Fe was removed with a magnetic stirring rod. The reaction mixture was concentrated and dried in vacuo to provide **C4** (0.50 g, 84 %) as an

bioRxiv preprint doi: https://doi.org/10.1101/038513; this version posted February 2, 2016. The copyright holder for this preprint (which was not certified by peer review) is the author/funder. All rights reserved. No reuse allowed without permission.

off-white solid, which was used for next step reaction without further purification. ESMS found *m/z* 247.1 ([M + H^+], $C_{11}H_7ClN_4O$ requires 246.0308), 269.0 [M + Na^+], 515.0 [2M + Na^+].

2-Chloro-5,11-dimethyl-5H-benzo[e]pyrimido[5,4-b][1,4]diazepin-6(11H)-one (C5). To a suspension of **C4** (0.50 g, 2.0 mmol) and MeI (0.30 mL, 4.8 mmol) in anhydrous DMF (10.0 mL) was added NaH (60%, 0.19 g, 4.8 mmol) at 0 ^oC under N_2. The reaction mixture was stirred at 0 ^oC for 10 min then warmed at 25 ^oC overnight. The reaction was quenched with 0.5 N HCl aqueous solution at 0 ^oC and stirred at 25 ^oC for additional 1 h. The precipitate was filtered, washed with 1 N HCl aqueous solution, H_2O, and hexanes, then dried in vacuo to provide **C3** as a solid (0.44 g, 80 %). ESMS found *m/z* 275.1 ([M + H^+], $C_{13}H_{11}ClN_4O$ requires 274.0621).

7-((2-Ethoxy-4-(4-(4-methylpiperazin-1-yl)piperidine-1-carbonyl)phenyl)amino)-5,10-dimethyl-5H-dipyrido[3,4-b:3',2'-e][1,4]diazepin-11(10H)-one (C6, AX15892). A mixture of **C5** (25 mg, 0.091 mmol), **C6** (34.7 mg, 0.100 mmol), K_2CO_3 (37.7 mg, 0.273 mmol), $Pd_2(dba)_3$ (5.0 mg, 0.0055 mmol), and X-Phos (3.8 mg, 0.0080 mmol) in ^{t}Butanol (1 mL) was purged with nitrogen gas several times, then was heated in a sealed vial at 100 ^oC overnight. At 25 ^oC, the reaction mixture was filtered through a short celite column, and washed with methanol. The filtrate was concentrated and the residue was purified by HPLC to obtain the product **C7** (**AX15892**, 2.07 mg, 95% purity, 3.9%) as a white powder. ^1H NMR (400 MHz, DMSO-d_6) δ ppm 1.27 - 1.43 (m, 2 H) 1.39 (t, *J* = 6.95 Hz, 3 H) 1.70 - 1.82 (m, 2 H) 1.86 (s, 4 H) 2.12 (s, 3 H) 2.18 - 2.36 (m, 4 H) 2.37 - 2.48 (m, 4 H) 3.27 (s, 3 H) 3.46 (s, 3 H) 4.14 (q, *J* = 6.82 Hz, 2 H) 6.91 (dd, *J* = 8.21, 1.64 Hz, 1 H) 6.98 (d, *J* = 1.77 Hz, 1 H) 7.03 (s, 1 H) 7.48 (dd, *J* = 8.46, 4.42

bioRxiv preprint doi: https://doi.org/10.1101/038513; this version posted February 2, 2016. The copyright holder for this preprint (which was not certified by peer review) is the author/funder. All rights reserved. No reuse allowed without permission.

Hz, 1 H) 7.72 (dd, *J* = 8.59, 1.01 Hz, 1 H) 8.21 (s, 1 H) 8.24 (s, 1 H) 8.32 (d, *J* = 8.34 Hz, 1 H) 8.37 (dd, *J* = 4.42, 1.14 Hz, 1 H); ESMS found *m/z* 585.0 ([M + H^+], $C_{32}H_{40}N_8O_3$ requires 584.3223).

Cell culture and live cell KiNativ™

Primary human umbilical vein endothelial cells (HUVECs) were grown in complete EGM-2 media (Lonza, Walkersville, MD) and used at passages 2-3. HeLa cells were kindly provided by Dr. Jiing-Dwan Lee (Scripps Research Institute, Department of Immunology, La Jolla, CA) and maintained in Eagles Minimum Essential Media (EMEM) containing 10% (v/v) charcoal-dextran treated, heat-inactivated FBS (Omega Scientific, Tarzana, CA), and 1x Penicillin/Streptomycin/Amphotericin B (Lonza, Walkersville, MD). The virally immortalized, normal human bronchial epithelial cell line BEAS-2B was purchased from ATCC (Manassas, VA) and grown in complete BEGM media (Lonza). All cells were grown at 37°C in a humidified atmosphere at 5% CO_2.

For determination of cellular kinase engagement, the KiNativ chemoproteomics platform was used. In live cell KiNativ, human PBMCs (Astarte Biologics, Bothell, WA) or Jurkat cells (ATCC) were incubated with compound for one hour at 37°C in a humidified atmosphere with 5% CO_2, washed, and collected for KiNativ analysis as previously described [24].

Detection of E-selectin

bioRxiv preprint doi: https://doi.org/10.1101/038513; this version posted February 2, 2016. The copyright holder for this preprint (which was not certified by peer review) is the author/funder. All rights reserved. No reuse allowed without permission.

HUVECs were pre-treated with compound or DMSO vehicle (0.1% final volume) in complete media for one hour at 37°C in a humidified atmosphere with 5% CO_2. Cells were then stimulated with 10 μg/mL Pam_3CSK_4 for 4 hrs. After brief trypsinization for detachment and dispersion, the cells were neutralized, filtered through a 40 micron cell strainer, and washed in cold flow cytometry staining buffer (FCSB)(eBioscience). Cells were incubated with 10 ug/mL human IgG in FCSB for 15 min on ice to block nonspecific Fc binding, and then incubated with 2.5 ug/mL fluorescein-anti-E-selectin antibody for 1 hr on ice. After washing, the cells were analyzed by flow cytometry on the Attune flow cytometer (Applied Biosystems/ThermoFisher Scientific). Pam_3CSK_4-stimulated, DMSO-treated cells incubated with a fluorescein-labeled, IgG_1 isotype control primary antibody were determined to exhibit no change in fluorescein signal relative to non-stimulated, DMSO-treated cells stained with the fluorescein-conjugated anti-E-selectin antibody, therefore the latter was used as the baseline control. Cells were first gated using forward vs side scatter, then 60,000 cells were analyzed for a gain in fluorescein signal relative to unstimulated DMSO-treated cells.

HeLa ERK5 auto-phosphorylation assay

HeLa cells were pre-treated with compound or DMSO vehicle in FBS-containing EMEM culture media and incubated for 1 h at 37°C in a humidified atmosphere at 5% CO_2. Compounds were tested in a 7-point serial dilution series ranging from 37.5 μM to 2.4 nM. Cells were left unstimulated or stimulated with 50 ng/mL EGF for 15 minutes then directly lysed in Laemmli sample buffer. Proteins in whole cell lysates were separated via SDS-polyacrylamide gel electrophoresis using 8% gels (Novex/ThemoFisher Scientific). ERK5 was detected by Western

bioRxiv preprint doi: https://doi.org/10.1101/038513; this version posted February 2, 2016. The copyright holder for this preprint (which was not certified by peer review) is the author/funder. All rights reserved. No reuse allowed without permission.

blot analysis using anti-human Erk5 polyclonal antibody and normalized to GAPDH or β-Actin. Phosphorylated ERK5 was observable as a slower migrating band. Fluorescent signal from the secondary detection antibodies was detected and quantified using the Odyssey Imaging System (LI-COR Biotechnology, Lincoln, NE). EC_{50} values were determined using GraphPad Prism software v5.04 (GraphPad Software, La Jolla, CA) after normalization to GAPDH or β-Actin.

Cytokine immunoanalyses

Cells in their respective growth media were seeded at 1-2 x 10^5 cells/well and allowed to adhere at 37°C in a humidified atmosphere with 5% CO_2. Cells were pre-treated with DMSO vehicle or compound in a 4-point serial dilution series from 10 to 0.08 μM for 1 h, after which cells were left unstimulated or stimulated with either 10 μg/mL Pam_3CSK_4 or 50 ng/mL IL-17A. Cells were incubated for 48 hours, after which the supernatant was collected for cytokine analyses. Cytokines were individually determined by ELISA (Life Technologies/ThermoFisher Scientific) or by multiplex immunoassay (Bio-Rad, Hercules, CA). ELISA absorbance was read at 450 nm using the Wallac 1420 Victor^2 multilabel microplate reader (Perkin Elmer, Waltham, MA), whereas fluorescence of multiplex magnetic beads was quantified using the Bio-Plex MAGPIX multiplex reader (Bio-Rad). EC_{50} values were determined using GraphPad Prism software, with cytokine levels from cells treated with DMSO + stimulation normalized as 100%, and nonstimulated concentrations set as 0%.

Preparation of cell samples for RNA-Seq

HUVEC or HeLa cells were plated in triplicate in 6-well tissue culture-coated dishes and allowed to adhere overnight. Cells were pre-incubated with DMSO vehicle (0.1% final concentration), 1

bioRxiv preprint doi: https://doi.org/10.1101/038513; this version posted February 2, 2016. The copyright holder for this preprint (which was not certified by peer review) is the author/funder. All rights reserved. No reuse allowed without permission.

μM AX15836 (ERK5 inhibitor), 5 μM AX15839 (dual ERK5/BRD inhibitor), or 1 μM I-BET762 (BRD inhibitor) for 1 hr. HUVEC and HeLa cells were then stimulated with their respective agonists (10 μg/mL Pam_3CSK_4 or 50 ng/mL EGF) for 5 hrs. Cells were processed to total RNA using the RNeasy kit (Qiagen, Valencia, CA). RNA was sent to the Scripps Research Next Generation Sequencing Core Facility (La Jolla, CA) for RNA-Seq.

One microgram total RNA from each sample was ribodepleted using the Ribo-Zero-rRNA Removal Kit (Epicentre, Madison, WI). Sequencing libraries were then prepared from ribodepleted RNA using NEBNext® Ultra™ RNA Library Prep Kit for Illumina following the manufacturer's recommended protocol and barcoded using standard Illumina TruSeq barcoded adapter sequences. Final libraries were size-selected using Agencourt AMPure XP beads. Purified libraries were pooled and loaded onto either an Illumina NextSeq500 sequencer for 75 base single end sequencing or an Illumina HiSeq2000 sequencer for 100 base single end sequencing with 7 base index read.

Genome Analyzer Pipeline Software (bcl2fastq ver.2.15.0.4) was used to perform image analysis, base calling, and demultiplexing. The program Cutadapt was used to trim the adapter and low base pair called scores. Per-exon gene counts were generated using TopHat2 software[45] and the HG19 release of the human genome. Raw count data analysis was performed using the Bioconductor software framework[46] and differential expression statistics were calculated using the DESeq2 package[47]. Genes differentially expressed in compound treated-samples vs. DMSO-treated samples were tabulated and results from both experiment sets were compared to each other using a cutoff of p-value levels less than 0.01.

bioRxiv preprint doi: https://doi.org/10.1101/038513; this version posted February 2, 2016. The copyright holder for this preprint (which was not certified by peer review) is the author/funder. All rights reserved. No reuse allowed without permission.

References

1. Morrison, D. K. MAP Kinase Pathways. *Cold Spring Harb. Perspect. Biol.* **4,** a011254 (2012).

2. Nithianandarajah-Jones, G. N., Wilm, B., Goldring, C. E. P., Müller, J. & Cross, M. J. ERK5: Structure, regulation and function. *Cell. Signal.* **24,** 2187–2196 (2012).

3. Mody, N., Campbell, D. G., Morrice, N., Peggie, M. & Cohen, P. An analysis of the phosphorylation and activation of extracellular-signal-regulated protein kinase 5 (ERK5) by mitogen-activated protein kinase kinase 5 (MKK5) in vitro. *Biochem. J.* **372,** 567–575 (2003).

4. Kondoh, K., Terasawa, K., Morimoto, H. & Nishida, E. Regulation of nuclear translocation of extracellular signal-regulated kinase 5 by active nuclear import and export mechanisms. *Mol. Cell. Biol.* **26,** 1679–1690 (2006).

5. Morimoto, H., Kondoh, K., Nishimoto, S., Terasawa, K. & Nishida, E. Activation of a C-terminal transcriptional activation domain of ERK5 by autophosphorylation. *J. Biol. Chem.* **282,** 35449–35456 (2007).

6. Diaz-Rodriguez, E. & Pandiella, A. Multisite phosphorylation of Erk5 in mitosis. *J. Cell Sci.* **123,** 3146–3156 (2010).

7. Iñesta-Vaquera, F. a. *et al.* Alternative ERK5 regulation by phosphorylation during the cell cycle. *Cell. Signal.* **22,** 1829–1837 (2010).

8. Honda, T. *et al.* Phosphorylation of ERK5 on Thr732 is associated with ERK5 nuclear localization and ERK5-dependent transcription. *PLoS One* **10,** e0117914 (2015).

9. English, J. M. Identification of substrates and regulators of the mitogen-activated protein kinase ERK5 using chimeric protein kinases. *J. Biol. Chem.* **273,** 3854–3860 (1998).

10. Kamakura, S., Moriguchi, T. & Nishida, E. Activation of the protein kinase ERK5/BMK1 by receptor tyrosine kinases: identification and chracterization of a signaling pathway to the nucleus. *J. Biol. Chem.* **274,** 26563–26571 (1999).

bioRxiv preprint doi: https://doi.org/10.1101/038513; this version posted February 2, 2016. The copyright holder for this preprint (which was not certified by peer review) is the author/funder. All rights reserved. No reuse allowed without permission.

11. Kato, Y. BMK1/ERK5 regulates serum-induced early gene expression through transcription factor MEF2C. *EMBO J.* **16,** 7054–7066 (1997).

12. Kasler, H. G., Victoria, J., Duramad, O. & Winoto, A. ERK5 is a novel type of mitogen-activated protein kinase containing a transcriptional activation domain. *Mol. Cell. Biol.* **20,** 8382–8389 (2000).

13. Sohn, S. J., Li, D., Lee, L. K. & Winoto, A. Transcriptional regulation of tissue-specific genes by the ERK5 mitogen-activated protein kinase. *Mol. Cell. Biol.* **25,** 8553–8566 (2005).

14. Yan, L. *et al.* Knockout of ERK5 causes multiple defects in placental and embryonic development. *BMC Dev. Biol.* **3,** 11 (2003).

15. Regan, C. P. *et al.* Erk5 null mice display multiple extraembryonic vascular and embryonic cardiovascular defects. *Proc. Natl. Acad. Sci.* **99,** 9248–9253 (2002).

16. Hayashi, M. *et al.* Targeted deletion of BMK1/ERK5 in adult mice perturbs vascular integrity and leads to endothelial failure. *J. Clin. Invest.* **113,** 1138–1148 (2004).

17. Koizumi, K. *et al.* Activation of p38 mitogen-activated protein kinase is necessary for gemcitabine-induced cytotoxicity in human pancreatic cancer cells. *Anticancer Res.* **25,** 3347–3353 (2005).

18. Pan, Y.-W. *et al.* Inducible and conditional deletion of extracellular signal-regulated kinase 5 disrupts adult hippocampal neurogenesis. *J. Biol. Chem.* **287,** 23306–23317 (2012).

19. Deng, X. *et al.* Discovery of a benzo[e]pyrimido-[5,4-b][1,4]diazepin-6(11H)-one as a potent and selective inhibitor of big MAP kinase 1. *ACS Med. Chem. Lett.* **2,** 195–200 (2011).

20. Yang, Q. *et al.* Pharmacological inhibition of BMK1 suppresses tumor growth through promyelocytic leukemia protein. *Cancer Cell* **18,** 258–267 (2010).

21. Bera, A. *et al.* A positive feedback loop involving Erk5 and Akt turns on mesangial cell proliferation in response to PDGF. *AJP Cell Physiol.* **306,** C1089–C1100 (2014).

22. Rovida, E. *et al.* The mitogen-activated protein kinase ERK5 regulates the development

bioRxiv preprint doi: https://doi.org/10.1101/038513; this version posted February 2, 2016. The copyright holder for this preprint (which was not certified by peer review) is the author/funder. All rights reserved. No reuse allowed without permission.

and growth of hepatocellular carcinoma. *Gut* **64,** 1454–1465 (2015).

23. Wilhelmsen, K., Mesa, K. R., Lucero, J., Xu, F. & Hellman, J. ERK5 protein promotes, whereas MEK1 protein differentially regulates, the toll-like receptor 2 protein-dependent activation of human endothelial cells and monocytes. *J. Biol. Chem.* **287,** 26478–26494 (2012).

24. Patricelli, M. P. *et al.* In situ kinase profiling reveals functionally relevant properties of native kinases. *Chem. Biol.* **18,** 699–710 (2011).

25. Patricelli, M. P. *et al.* Functional interrogation of the kinome using nucleotide acyl phosphates. *Biochemistry* **46,** 350–358 (2007).

26. Kato, Y. *et al.* Bmk1/Erk5 is required for cell proliferation induced by epidermal growth factor. *Nature* **395,** 713–6 (1998).

27. Peebles, Jr., R. S., Bochner, B. S. & Schleimer, R. P. in *Inflammation: Mediators and Pathways* (eds. Ruffolo, Jr., R. R. & Hollinger, M. A.) (CRC Press, Inc., 1995).

28. Martin, M. P., Olesen, S. H., Georg, G. I. & Schönbrunn, E. Cyclin-dependent kinase inhibitor dinaciclib interacts with the acetyl-lysine recognition site of bromodomains. *ACS Chem. Biol.* **8,** 2360–2365 (2013).

29. Ember, S. W. J. *et al.* Acetyl-lysine binding site of bromodomain-containing protein 4 (BRD4) interacts with diverse kinase inhibitors. *ACS Chem. Biol.* **9,** 1160–1171 (2014).

30. Ciceri, P. *et al.* Dual kinase-bromodomain inhibitors for rationally designed polypharmacology. *Nat. Chem. Biol.* **10,** 305–312 (2014).

31. Filippakopoulos, P. *et al.* Selective inhibition of BET bromodomains. *Nature* **468,** 1067–1073 (2010).

32. Mirguet, O. *et al.* Discovery of epigenetic regulator I-BET762: lead optimization to afford a clinical candidate inhibitor of the BET bromodomains. *J. Med. Chem.* **56,** 7501–7515 (2013).

33. Nicodeme, E. *et al.* Suppression of inflammation by a synthetic histone mimic. *Nature* **468,** 1119–1123 (2010).

bioRxiv preprint doi: https://doi.org/10.1101/038513; this version posted February 2, 2016. The copyright holder for this preprint (which was not certified by peer review) is the author/funder. All rights reserved. No reuse allowed without permission.

34. Wu, L. *et al.* A novel IL-17 signaling pathway controlling keratinocyte proliferation and tumorigenesis via the TRAF4-ERK5 axis. *J. Exp. Med.* **212,** 1571–1587 (2015).

35. Laan, M., Lötvall, J., Chung, K. F. & Lindén, A. IL-17-induced cytokine release in human bronchial epithelial cells in vitro: role of mitogen-activated protein (MAP) kinases. *Br. J. Pharmacol.* **133,** 200–206 (2001).

36. Chesné, J. *et al.* IL-17 in severe asthma. Where do we stand? *Am. J. Respir. Crit. Care Med.* **190,** 1094–1101 (2014).

37. Kawaguchi, M. *et al.* Modulation of bronchial epithelial cells by IL-17. *J. Allergy Clin. Immunol.* **108,** 804–809 (2001).

38. Wilhelmsen, K. *et al.* Extracellular signal-regulated kinase 5 promotes acute cellular and systemic inflammation. *Sci. Signal.* **8,** ra86–ra86 (2015).

39. Amit, I. *et al.* A module of negative feedback regulators defines growth factor signaling. *Nat. Genet.* **39,** 503–512 (2007).

40. Finegan, K. G. *et al.* ERK5 is a critical mediator of inflammation-driven cancer. *Cancer Res.* **75,** 742–753 (2015).

41. Weiss, W. A., Taylor, S. S. & Shokat, K. M. Recognizing and exploiting differences between RNAi and small-molecule inhibitors. *Nat. Chem. Biol.* **3,** 739–744 (2007).

42. Belkina, A. C., Nikolajczyk, B. S. & Denis, G. V. BET protein function is required for inflammation: Brd2 genetic disruption and BET inhibitor JQ1 impair mouse macrophage inflammatory responses. *J. Immunol.* **190,** 3670–3678 (2013).

43. Schaefer, U. Pharmacological inhibition of bromodomain-containing proteins in inflammation. *Cold Spring Harb. Perspect. Biol.* **6,** (2014).

44. Klein, K. *et al.* The bromodomain protein inhibitor I-BET151 suppresses expression of inflammatory genes and matrix degrading enzymes in rheumatoid arthritis synovial fibroblasts. *Ann. Rheum. Dis.* 1–8 (2014). doi:10.1136/annrheumdis-2014-205809

45. Kim, D. *et al.* TopHat2: accurate alignment of transcriptomes in the presence of insertions, deletions and gene fusions. *Genome Biol.* **14,** R36 (2013).

bioRxiv preprint doi: https://doi.org/10.1101/038513; this version posted February 2, 2016. The copyright holder for this preprint (which was not certified by peer review) is the author/funder. All rights reserved. No reuse allowed without permission.

46. Huber, W. *et al.* Orchestrating high-throughput genomic analysis with Bioconductor. *Nat. Methods* **12,** 115–121 (2015).

47. Love, M. I., Huber, W. & Anders, S. Moderated estimation of fold change and dispersion for RNA-seq data with DESeq2. *Genome Biol.* **15,** 550 (2014).

bioRxiv preprint doi: https://doi.org/10.1101/038513; this version posted February 2, 2016. The copyright holder for this preprint (which was not certified by peer review) is the author/funder. All rights reserved. No reuse allowed without permission.

Supplementary Information is linked to the online version of the paper at www.nature.com/nature.

Supplementary Results

Supplementary Data 1. KiNativ profile of compounds screened at 1 μM in Jurkat cell lysate.

Supplementary Data 2. KiNativ profile of compounds screened at 10 μM in Jurkat cell lysate.

Supplementary Table 1. Comparative efficacy of an ERK5-specific inhibitor and a BRD-specific inhibitor in cell models of innate and adaptive immunity

bioRxiv preprint doi: https://doi.org/10.1101/038513; this version posted February 2, 2016. The copyright holder for this preprint (which was not certified by peer review) is the author/funder. All rights reserved. No reuse allowed without permission.

Acknowledgements

We express gratitude to our colleague and friend, the late Dr. Kevin Shreder for his invaluable contributions to this work. We thank Kai Nakamura, Lan Pham, Ray Li, and Julia Ayers for their assistance in chemical syntheses.

Author Contributions

E.C.K.L., C.M.A., and J.I. developed and performed cell-based assays; T.K.N. planned and analyzed KiNativ studies. H.W. analyzed the RNA-Seq results. K.S., Y.H., S.S., and B.L. designed and synthesized inhibitors. E.C.K.L, T.K.N., H.W., Y.H., J.W.K., and J.S.R. wrote the paper.

Author Information

Reprints and permissions information is available at www.nature.com/reprints.

Correspondence and requests for materials should be addressed to E.C.K.L.: emmel@activx.com

Competing Financial Interests

E.C.K.L, C.M.A., T.K.N., H.W., Y.H., S.S., B.L., J.W.K., and J.S.R. , employees of ActivX Biosciences, a wholly owned subsidiary of Kyorin Pharmaceutical Co., Ltd. , and J.I., an employee of Kyorin Pharmaceutical Co., Ltd., have commercial interests in the development of ERK5 and BRD inhibitors.

bioRxiv preprint doi: https://doi.org/10.1101/038513; this version posted February 2, 2016. The copyright holder for this preprint (which was not certified by peer review) is the author/funder. All rights reserved. No reuse allowed without permission.

Table 1. Surface E-selectin expression on endothelial cells stimulated with TLR1/2 agonist Pam_3CSK_4.

Condition	E-selectin Expression (% of cell population)	Percent Inhibition
DMSO	17.2	0
AX15836	18.5	0
AX15839	13.7	21
AX15892	18.1	0
AX15910	12.8	27
XMD8-92	10.9	38

HUVECs were pre-treated with 10 μM of compound prior to stimulation with 10 μg/mL Pam_3CSK_4 for 4 hrs. E-selectin expression was detected and quantified by flow cytometry. Unstimulated cells expressed a baseline E-selectin expression of 0.6%. Shown are results from a representative experiment from at least 2 independent experiments.

bioRxiv preprint doi: https://doi.org/10.1101/038513; this version posted February 2, 2016. The copyright holder for this preprint (which was not certified by peer review) is the author/funder. All rights reserved. No reuse allowed without permission.

Table 2. Inhibitor characteristics and classification.

Compound	**ERK5 IC_{50} (nM)[a]**	**BRD4(1) K_d (nM)[b]**	**Ratio of ERK5 IC_{50}:BRD4(1) K_d**	**Inhibitor Classification**
AX15836	8	3600	0.002	ERK5
AX15892	30	610	0.049	ERK5
AX15839	170	130	1.3	Dual
AX15910	20	22	0.9	Dual
XMD8-92	190	170	1.1	Dual
I-BET762	>10000	31	>320	BRD
JQ1	>10000	6	>1670	BRD

[a]ERK5 IC_{50} value determined using KiNativ

[b]BRD4(1) K_d value determined at DiscoveRx

bioRxiv preprint doi: https://doi.org/10.1101/038513; this version posted February 2, 2016. The copyright holder for this preprint (which was not certified by peer review) is the author/funder. All rights reserved. No reuse allowed without permission.

Table 3: EC_{50} values of compounds in reducing cytokines IL-6 and IL-8 produced by endothelial cells stimulated with TLR1/2 agonist Pam_3CSK_4.

Compound	Inhibitor Classification	EC_{50} (μM) of cytokine reduction	
		IL-6	IL-8
AX15836	ERK5	>>10	>>10
AX15839	Dual	1.73	1.79
I-BET762	BRD	0.15	0.12

HUVECs were pre-treated with compound prior to stimulation with 10 μg/mL Pam_3CSK_4 for 48 hrs. Culture supernatants were tested for cytokines by immunoassay. Shown are results from a representative experiment from at least 2 independent experiments.

bioRxiv preprint doi: https://doi.org/10.1101/038513; this version posted February 2, 2016. The copyright holder for this preprint (which was not certified by peer review) is the author/funder. All rights reserved. No reuse allowed without permission.

Table 4: EC_{50} values of compounds in reducing cytokines IL-6 and IL-8 produced by bronchial epithelial cells stimulated with IL-17A.

Compound	**Inhibitor Classification**	**EC_{50} (μM) of cytokine reduction**	
		IL-6	**IL-8**
AX15836	ERK5	>>10	>>10
AX15839	Dual	1.13	1.07
I-BET762	BRD	0.16	0.07

BEAS-2B cells were pre-treated with compound prior to stimulation with 50 ng/mL IL-17A for 48 hrs. Culture supernatants were tested for cytokines by immunoassay. Shown are results from a representative experiment from at least 2 independent experiments.